Acta Oceanol. Sin., 2019, Vol. 38, No. 12, P. 1–7
https://doi.org/10.1007/s13131-019-1508-1
http://www.hyxb.org.cn
E-mail: hyxbe@263.net

Distributions of $^{224, 223}$Ra and ^{137}Cs in the Luzon Strait and its adjacent waters and their response to Typhoon Rainbow

Hequan Gu[1]*, Feng Zhao[1], Wei Yu[1], Ruihuan Li[2], Li Zhao[1], Dongmei Li[1]

[1] South China Sea Environment Monitoring Center, State Oceanic Administration, Guangzhou 510300, China

[2] State Key Laboratory of Tropical Oceanography, South China Sea Institute of Oceanology, Chinese Academy of Sciences, Guangzhou 510301, China

Received 8 May 2019; accepted 29 July 2019

Abstract

This paper reports the distribution of natural radionuclides of $^{224, 223}$Ra in the surface water and stratified waters of the Luzon Strait and its adjacent waters during the cruises of September 2015 and May 2016. To understand the impact of the Fukushima nuclear accident, the artificial radionuclide ^{137}Cs in the waters was also analyzed. The results showed that the activities of $^{224, 223}$Ra and ^{137}Cs were all within the natural radioactive background levels of the marine environment in the South China Sea. ^{224}Ra had a higher activity level in the water of the north South China Sea to the west of the Luzon Strait, and a lower activity level in the oceanic Philippine Sea to the east. The ^{137}Cs activity had no obvious spatial trends. Based on the vertical trends of ^{224}Ra, ^{137}Cs, and water temperature and salinity at three stations (LS3, LS5 and LS8), the distinct characteristics of the activity levels and gradients of ^{224}Ra and ^{137}Cs among the tropical surface water, subsurface water and mid-deep water were revealed. Typhoon Rainbow event reversed the overall circulation of the Luzon Strait and its adjacent area. A huge amount of western Pacific water characterized by low ^{224}Ra activities flooded into the South China Sea, reducing the activity level of ^{224}Ra in the waters. However, there were no significant differences of ^{137}Cs activity between the West Pacific and the north South China Sea, and ocean current changes had no effect on the ^{137}Cs activity levels of the water bodies.

Key words: ^{224}Ra, ^{223}Ra, Luzon Strait, typhoon, ^{137}Cs

Citation: Gu Hequan, Zhao Feng, Yu Wei, Li Ruihuan, Zhao Li, Li Dongmei. 2019. Distributions of $^{224, 223}$Ra and ^{137}Cs in the Luzon Strait and its adjacent waters and their response to Typhoon Rainbow. Acta Oceanologica Sinica, 38(12): 1–7, doi: 10.1007/s13131-019-1508-1

1 Introduction

The Fukushima nuclear accident in Japan was the first major accident that seriously affected the safety of the marine environment and marine ecosystem since the beginning of peaceful use of nuclear energy. The total amount of ^{137}Cs directly discharged into the western Pacific by the Fukushima accident is reported by some scholars to be as high as (27±15) PBq (Bailly du Bois et al., 2012). The radioactive wastewater discharged by the nuclear accident migrates and spreads under the transport of ocean currents, which may pose a threat to the ecological environment of the South China Sea.

The Luzon Strait is the most important channel for water exchange between the South China Sea and the western Pacific. However, the dynamic process of the western Pacific water current flowing through the Luzon Strait is very complex. Therefore, our understanding of the impact of the Fukushima accident on the marine ecological environment of the South China Sea has been greatly limited by the difficulties of evaluating the exchange capacity between the western Pacific and the South China Sea, and analyzing the transport and diffusion of the radiation pollution from Fukushima accident into the South China Sea. Some information useful for addressing this scientific issue may be provided by using natural radioactive isotopes of radium. Two natural short half-life radium isotopes exist in the marine environment, namely ^{224}Ra ($t_{1/2}$=3.7 d) and ^{223}Ra ($t_{1/2}$=11.4 d). Both of these are dissolved nuclides, which can be used as good tracers for studying ocean current and water mass mixing processes in oceanographic research (Moore, 2000; Moore and Krest, 2004; Hancock et al., 2006; Dulaiova and Burnett, 2008; Stachelhaus et al., 2012).

In this study, the radioactivity levels of ^{224}Ra and ^{223}Ra in the Luzon Strait and its adjacent waters were observed, and the horizontal and vertical distribution characteristics of both radium isotopes were evaluated, which provides basic data and theoretical support for subsequent tracer applications. The artificial radionuclide ^{137}Cs ($t_{1/2}$=30.17 a), which is one of the most important nuclides produced by nuclear fission and is generally used to indicate the level and extent of marine radioactive contamination (Bailly du Bois et al., 2012; Charette et al., 2013; Aoyama et al., 2016; Zhou et al., 2018; Buesseler et al., 2018), was also analyzed. Moreover, this study attempted to utilize satellite altimeter data to explore the impact of the strong Typhoon Rainbow event on the radioisotope distribution and migration behavior in the study area. The results of this study may be helpful for scientific

Foundation item: The Natural Science Foundation of Guangdong Province of China under contract No. 2017A030310592; the Open Project of State Key Laboratory of Tropical Oceanography, South China Sea Institute of Oceanology, Chinese Academy of Sciences under contract No. LTO1709; the Key Program of Bureau Director of State Oceanic Administration, P.R. China under contract No.180104.

*Corresponding author, E-mail: guhequan1983@163.com

evaluation of water exchange across the Luzon Strait and its impact on distributions of radium and cesium isotopes.

2 Study area

The Luzon Strait is located between the Taiwan Island of China and the Luzon Island of the Philippines. It spans three degrees of latitude, extends in the east-west direction, has a width of 380 km from north to south, and has an average water depth of 1 400 m. It consists of three straits and their waterways: the northern Bass Strait, the central Balintang Strait and the southern Babuyan Strait. The Luzon Strait is the only channel directly connecting the South China Sea and the Northwest Pacific Ocean, and its hydrodynamic process is greatly controlled by the famous Kuroshio Current. Within the Luzon Strait variable zonal currents exist throughout the year. The depth of the zonal flow into and out of the South China Sea is typically around 500 m. Generally, the inflow from the ocean into the strait, with an average monthly discharge of 10×10^6 m^3/s, is located in the central and southern parts of the strait. The outflow is located in the northern part of the strait, and its average monthly flow rate is 5×10^6 m^3/s (Liu et al., 2000).

3 Sample collection and analysis

3.1 *Field observation and sampling*

In the periods of September 2015 and May 2016, two voyages were carried out to investigate the activities of $^{224,\ 223}$Ra and ^{137}Cs in the Luzon Strait and its surrounding waters. The sampling stations of surface seawater are shown in Fig. 1. To investigate the vertical distribution trend of ^{224}Ra and ^{137}Cs in the study area, vertical water samples were collected at three stations (LS3, LS5 and LS8) during the cruise in May 2016. The stratified samples (total of 24) were collected from depths of roughly 0, 50, 100, 150, 200, 500, 600, 1 000 and 1 500 m.

The surface samples were pumped with a submerged pump and the stratified samples were collected by a Niskin multi-bottle water sampler. The shipborne CTD system acquired hydrological parameters such as temperature and salinity at the period of sampling. Compared with those of nearshore samples, the offshore activities of radium isotopes were usually quite low, and so the water volume for radium collection was increased from routine 60 L to 120–200 L. Upon return to the onboard laboratory, the water samples were immediately filtered using filtration cartridges (pore size: 0.5 μm) to separate the particulate and dissolved phases of the radionuclides. The filtered water was passed through a column filled with 20 g of MnO_2-impregnated acrylic fiber at a flow rate of approximately 0.5 L/min to ensure quantitative radium adsorption (Moore, 1976). Then, the residual water of the Mn-fibers was extracted by a vacuum pump, and the fibers were washed with deionized water 1–2 times to remove the salt covering the fibers. The humidity of the fibers was controlled to about 0.75 (water/manganese fiber mass ratio) (Garcia-Solsona et al., 2008).

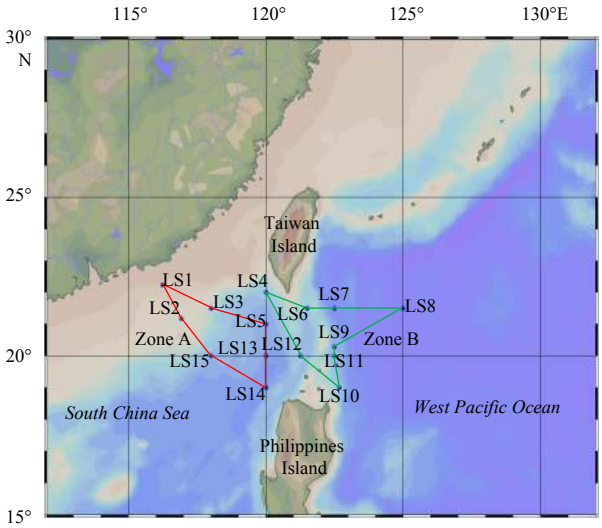

Fig. 1. Sampling stations in the Luzon Strait and its adjacent areas for both of the cruises of September 2015 and May 2016. Red lines show Zone A sampled before the Rainbow typhoon occurring in the cruise of September 2015; green lines show Zone B sampled after Typhoon Rainbow; and both zones were also sampled in the cruise of May 2016.

3.2 *Analysis method*

The amount of ^{224}Ra and ^{223}Ra collected on the Mn-fibers was measured using a Radium Delayed Coincidence Counter (Moore and Arnold, 1996). After the on-site sample collection, the gaseous daughter of ^{220}Rn generated by ^{224}Ra was carried by high-purity helium and entered into the Lucas scintillation chamber as soon as possible in order to record the count. Based on design principles of RaDeCC, high ^{224}Ra activity would interfere with the measurement of ^{223}Ra, therefore, ^{223}Ra counts were determined after 7–12 d of sample collection (about three ^{224}Ra half-life periods). The Mn-fibers were then stored for 6 weeks and measured again to obtain the supported ^{224}Ra from its parent, ^{228}Th. The uncertainties of the ^{224}Ra and ^{223}Ra activities were estimated to be 5%–20% and 30%–70%, respectively, using the equations derived by Garcia-Solsona et al. (2008).

The activities of ^{137}Cs in seawater were measured using a high-purity gamma ray spectrometer (model: BE5030, Canberra, USA). The 60 L of seawater was collected and acidified by adding 1 mL of concentrated hydrochloric acid per liter. Upon return to the terrestrial laboratory, 30 mg of hydrazine carrier was added. ^{137}Cs was co-precipitated with 12 g of solid ammonium phosphomolybdate (AMP) reagent. The ^{137}Cs activity was determined at 661.6 keV (85.1%). The detector efficiencies were calibrated using efficiency curves obtained from LabSOCS (Bronson, 2003). The chemical yield of this method was around 80%.

3.3 *Geostrophic flow data*

The Archiving, Validation and Interpolation of Satellite Oceanographic (AVISO) satellite altimeter data (ftp-access.aviso.altimetry.fr) were used to study the ocean flow field in the study area. The spatial resolution of the data was (1/4)° and the time resolution was 7 d. The data were combined with several satellite data such as TOPEX/POSEIDON, JASON-1, ERS-1/2, and Envisat, and the accuracy was greatly improved. The time scales of the data were 22–28 September 2015, 8–14 October 2015, and 21–27 May 2016, and the spatial ranges were 15°–30°N, 112°–132°E.

3.4 *Typhoon data*

The typhoon path data were obtained from the Unisys climate website of the Joint Typhoon Warning Center (JTWC) (http://weather.unisys.com). The data provided by the website includes the latitude and longitude of the typhoon center, and the maximum sustained wind speed and typhoon grade every 6 h.

4 Results and discussion

4.1 *Horizontal distributions of ^{224}Ra and ^{137}Cs*

Based on the results of two surveys, the activity of ^{224}Ra in surface water of the Luzon Strait and its adjacent waters ranged from 0.017 to 0.358 mBq/L, with an average of (0.132±0.093) mBq/L; the activity of ^{223}Ra ranged from undetected to 0.013 mBq/L, with an average value of (0.002±0.003) mBq/L. Compared with the relevant data ranging from 0.2 to 14 mBq/L for ^{224}Ra and from 0.03 to 1.3 mBq/L for ^{223}Ra in near-shore waters such as the Hainan Island and Changjiang Estuary (Gu, 2015), the activities of ^{224,223}Ra in the Luzon Strait and its surrounding water bodies were at an extremely low level.

The activity of ^{137}Cs in surface water of the Luzon Strait and its adjacent waters ranged from 0.58 to 1.27 mBq/L, with an average of (0.91±0.17) mBq/L. Compared with the average value of (1.12±0.08) mBq/L for ^{137}Cs activity reported by Wu et al. (2012), the activity level reported in this study was slightly lower, possibly because the study area is in the open ocean, where the ^{137}Cs level is often lower than it is in the near-shore area. In the study area, the activity of ^{137}Cs was within the background level of radioactivity in the marine environment of the South China Sea.

Because the ^{223}Ra activity was quite low and not detected in some samples, we only discuss the data of ^{224}Ra and ^{137}Cs collected in this study. The horizontal distribution of ^{224}Ra and ^{137}Cs in the surface water of the Luzon Strait and its adjacent waters are shown in Fig. 2. During these two investigations, the ^{224}Ra showed a higher activity in the north South China Sea to the west of the Luzon Strait and a lower activity in the Philippine Sea to the east of the Luzon Strait. The highest value that appeared in the study area was in the northwestern part of the area near the Luzon Island, followed by the area near the Dongsha Islands. The lowest value, a very low ^{224}Ra activity level (0.017 mBq/L), appeared in the Philippine Sea near the area northeast of Luzon Island. Considering that the ^{224}Ra in the distant ocean is derived mainly from the diffusion of near-shore water to the sea, the spatial characteristic of ^{224}Ra showed a typical distribution in the ocean.

^{137}Cs has a long half-life ($t_{1/2}$=30.17 a) and its distribution characteristics is not similar with that of ^{224}Ra. During the cruise of September 2015, as shown in Fig. 2c, the highest ^{137}Cs activity was observed in the northeastern part of the area near the Luzon Island (LS11), followed by the area near the Dongsha Islands (LS3); the lowest value was observed in the southwestern part of the zone near the Taiwan Island (LS4). During the cruise of May 2016, as shown in Fig. 2d, the maximum value was observed in the coast near the main land of China (LS1), followed by the middle part of the Luzon Strait (LS12); the minimum was observed in the middle of the South China Sea (LS15). The ^{137}Cs distribution in the study area was relatively scattered and complex (Fig. 2c and d). Therefore, it is quite difficult to summarize distinct spatial characteristics of ^{137}Cs in the study area.

4.2 *Vertical distributions of ^{224}Ra and ^{137}Cs*

From the cruise of May 2016, Figs 3a and b show the vertical distribution of temperature and salinity at three stations (LS3, LS5 and LS8) in water depths shallower than 1 800 m. The mixed layer thickness at the three stations was about 50 m, and the thermocline, through which temperature decreased from 28°C to about 5°C, began at a depth of about 100 m. The salinity of the

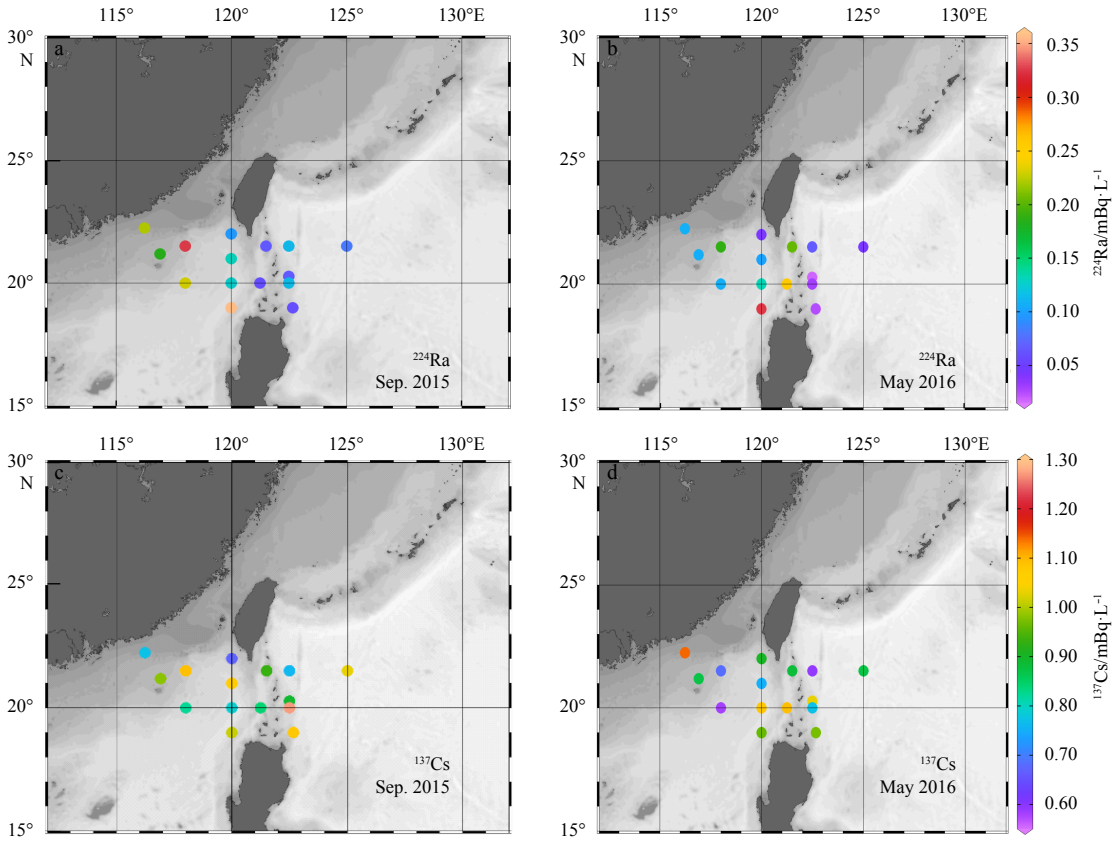

Fig. 2. Horizontal distributions of ^{224}Ra and ^{137}Cs activities in the Luzon Strait and its adjacent areas during the cruises of September 2015 and May 2016.

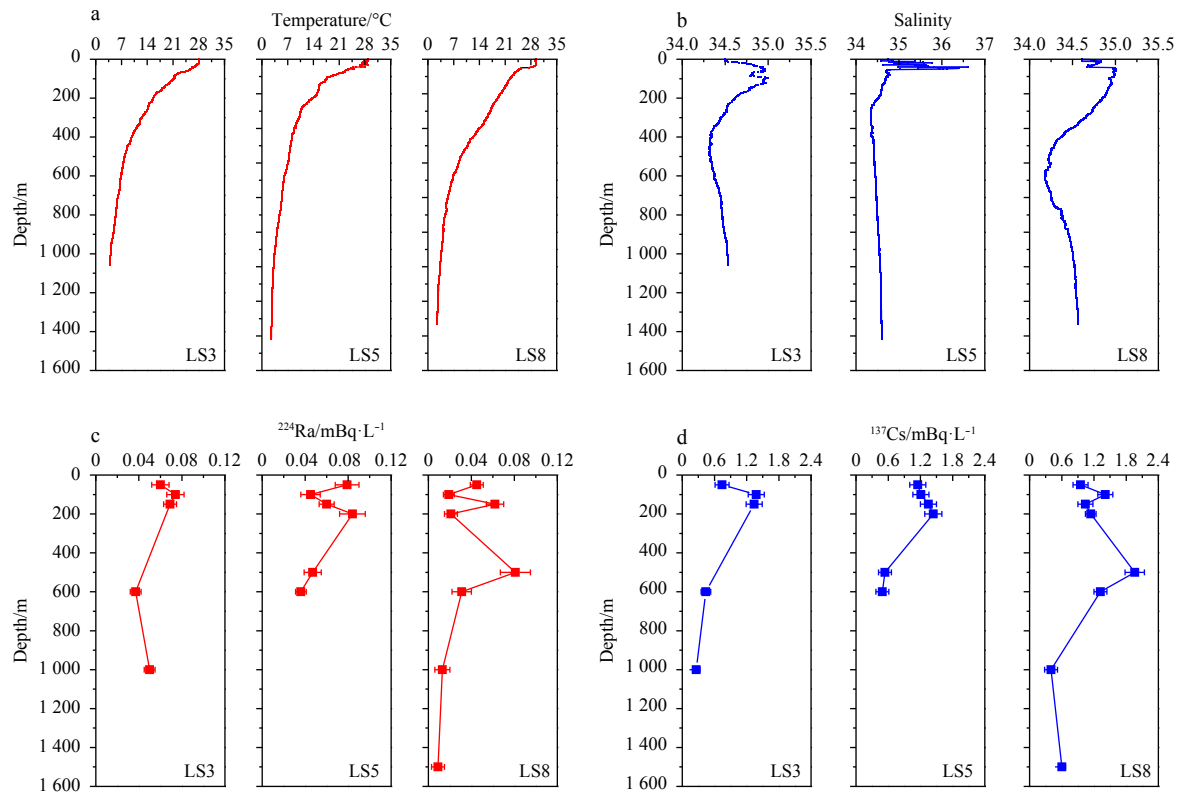

Fig. 3. Vertical distributions of water temperature (°C), salinity, ^{224}Ra, and ^{137}Cs (mBq/L) at Stas LS3, LS5 and LS8 during the cruise of May 2016

surface layer and the subsurface layer varied sharply. Specifically, the salinity increased dramatically and reached a maximum value at a water depth of about 100 m. Then, the salinity at Stas LS3, LS5, and LS8 decreased sharply from the water depth of 100 m to 400 m, 300 m, and 700 m, respectively. After reaching their minimum values of 34.3 (LS3 and LS5) and 34.2 (LS8), respectively, water salinity gradually increased to around 34.5. According to hydrological characteristics of offshore water masses in China summarized by Pan et al. (2005), the water layer where the minimum salinity occurred at the Philippine Sea is 100–300 m deeper than that of the South China Sea. Therefore, based on the water depths where the three stations reached the minimum values of salinity, it can be preliminarily determined that Stas LS3 and LS5 have the typical water feature of the South China Sea, while Sta. LS8 possessed the obvious seawater characteristics of the West Pacific Ocean.

The vertical distributions of ^{224}Ra and ^{137}Cs activities at the three stations are shown in Figs 3c and d. The ^{224}Ra activities of the stratified samples at Stas LS3 and LS5 fluctuated within the range of 0.036–0.084 mBq/L. Compared with those of Stas LS3 and LS5, the vertical activity of ^{224}Ra at Sta. LS8 was relatively low, but the vertical variation was more obvious, ranging from 0.009 to 0.081 mBq/L. The variation range of ^{137}Cs activity at Stas LS3 and LS5 was 0.26–1.44 mBq/L, but Sta. LS8 had larger variation of ^{137}Cs activity, ranging from 0.4 to 1.96 mBq/L. On the whole, the vertical distribution of ^{224}Ra activity was generally similar to that of ^{137}Cs activity within the limits of measurement error, especially at Sta. LS8. Specifically, the activities of ^{224}Ra and ^{137}Cs at Sta. LS8 increased to their maximum values at the water depth of 600 m and then gradually decreased to their minimum values. This phenomenon is discussed in the next section.

4.3 *^{224}Ra and ^{137}Cs activities in three water masses*

The scatter plots of ^{224}Ra and ^{137}Cs activities in T-S space for all samples are shown in Fig. 4, in which the symbol color represents the activity of ^{224}Ra or ^{137}Cs. The T-S curves of ^{224}Ra and ^{137}Cs showed an anti-S-shape characteristic, which is consistent with the typical hydrological characteristics in the study area. Based on conclusions of vertical water mass analysis (Pan, 2005), the study area can be divided into the tropical surface water (TSW, 0–50 m), the subsurface water (SSW, 50–300 m), and the intermediate and deep water (I&DW, >300 m), and then this categorization was used to delineate the water masses on Fig. 4.

The temperature of TSW remained relatively stable within the range of 27.2–30.7°C, while the water salinity varied from 33.5 to 34.8. The TSW had a higher activity of ^{224}Ra, and a significant gradient variation of ^{224}Ra activity, i.e., 0.017–0.358 mBq/L. ^{137}Cs activities were much lower in the TSW than the other two water masses, and most of them were concentrated between 0.58 and 1.09 mBq/L. By contrast, the SSW temperature had a large range of 15.0–25.9°C, but the salinity of SSW remained relatively consistent within the range of 34.6–35.9. ^{224}Ra activities of the SSW had much lower values with the range of 0.019–0.084 mBq/L, while the activity gradient of ^{137}Cs was more significant, varying from 0.74–1.44 mBq/L. The characteristics of I&DW were roughly consistent with those of the SSW. In particular, water temperature had large variation and salinity remained stable, ranging from 2.6–10.8°C and 34.2–34.6, respectively. The I&DW had relatively consistent ^{224}Ra activity with a range of variation of 0.009–0.084 mBq/L, while ^{137}Cs in I&DW had a larger range from 0.26 to 1.96 mBq/L.

During May 2016, high activity values of ^{224}Ra and ^{137}Cs appeared at Sta. LS8 at a depth of 600 m (Figs 3a, b), and these were

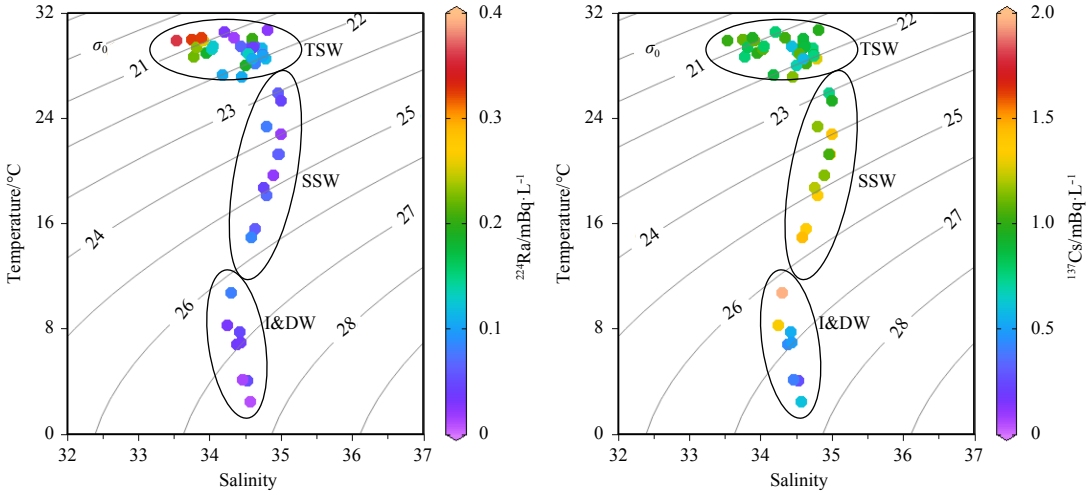

Fig. 4. Scatter plots of ^{224}Ra and ^{137}Cs activities versus water temperature and salinity in the study area. Color bars indicate the activities of ^{224}Ra and ^{137}Cs. The circles show the classification by water depth of three water masses, which are tropical surface water (TSW, 0–50 m), subsurface water (SSW, 50–300 m), and intermediate water and deep water (I&DW, >300 m), respectively.

significantly higher than those at the same water depth at Stas LS3 and LS5. However, the high values were not apparent in the T-S scatter plot of ^{224}Ra and ^{137}Cs (Fig. 4), which indicated that Sta. LS8 located in the Philippine Sea might have subsurface water characterized by high activities of ^{224}Ra and ^{137}Cs submerged into layers of the intermediate water and deep water and that the mixing process might then increase the activity levels of both radionuclides.

4.4 *Influence of Typhoon Rainbow on ^{224}Ra and ^{137}Cs activities*

4.4.1 *Typhoon Rainbow*

Typhoon Rainbow, the No. 22 typhoon in 2015, strengthened from a tropical depression to a tropical storm when it crossed the Luzon Island at 02:00 on October 2. Figure 5 shows the path of Typhoon Rainbow. It then entered the northeastern part of the South China Sea and continued to move northwestward with increasing intensity. At 14:00 on October 3, it was upgraded to a typhoon level, and then at 23:00 upgraded a strong typhoon level, with a central air pressure of 955 hPa and a central wind speed of 45 m/s. It was further upgraded as a strong typhoon and landed on the coast of Zhanjiang, Guangdong Province, at 14:00 on October 4. The maximum wind speed was 50 m/s. Since the founding of the country, Typhoon Rainbow was the strongest typhoon to make landfall in China.

4.4.2 *Variation of sea currents led by Typhoon Rainbow*

Based on the AVISO satellite altimeter data, the geostrophic flow fields in the study area were calculated before and after the typhoon event, respectively, as shown in Fig. 6. Before the formation of Typhoon Rainbow in late September 2015, there was a significant eastward current in the central part of the Luzon Strait, that is, sea water of the northern South China Sea flowed into the Philippine Sea in the form of an anticyclone, mixed with the Kuroshio water and then bypassed the Luzon Strait, entering the western Pacific Ocean along the eastern side of Taiwan Island. After the end of the typhoon in mid-October, the eastward current disappeared. One part of the Kuroshio water flowed into the South China Sea in the form of a cyclone, and the other part continued to enter the western Pacific Ocean along the east side of

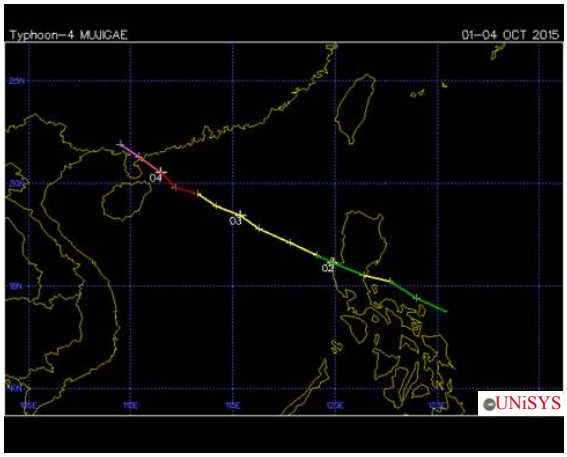

Fig. 5. Path map of Typhoon Rainbow, and typhoon grades are indicated by line colors (green: tropical depression, yellow: tropical storm, red: Typhoon-1, orange: Typhoon-2, and pink: Typhoon-4).

Taiwan Island. In brief, the surface ocean circulation around the Luzon Strait had undergone an overall reversal after Typhoon Rainbow event. In May 2016, the geostrophic flow field in the study area was roughly similar to that in mid-October 2015, but the intensity of the cyclone, which was formed by the northern South China Sea water merging with the influx of Kuroshio water, was much stronger. The major part of the interflow returned to the South China Sea in the form of a cyclone, while the other part bypassed the Luzon Strait northward along the eastern side of Taiwan Island, entering the western Pacific Ocean.

4.4.3 *Impact of Typhoon Rainbow on activities of ^{224}Ra and ^{137}Cs in the surface water*

To avoid the effects of Typhoon Rainbow, we were forced to return to port for more than 10 d during the cruise of September 2015. Thus, the survey was divided into two sampling stages: “before typhoon” and “after typhoon”, which had the durations of 22–27 September 2015 and 8–11 October 2015, respectively. As shown in Fig. 1, Zone A indicated by red lines indicates the "pre-

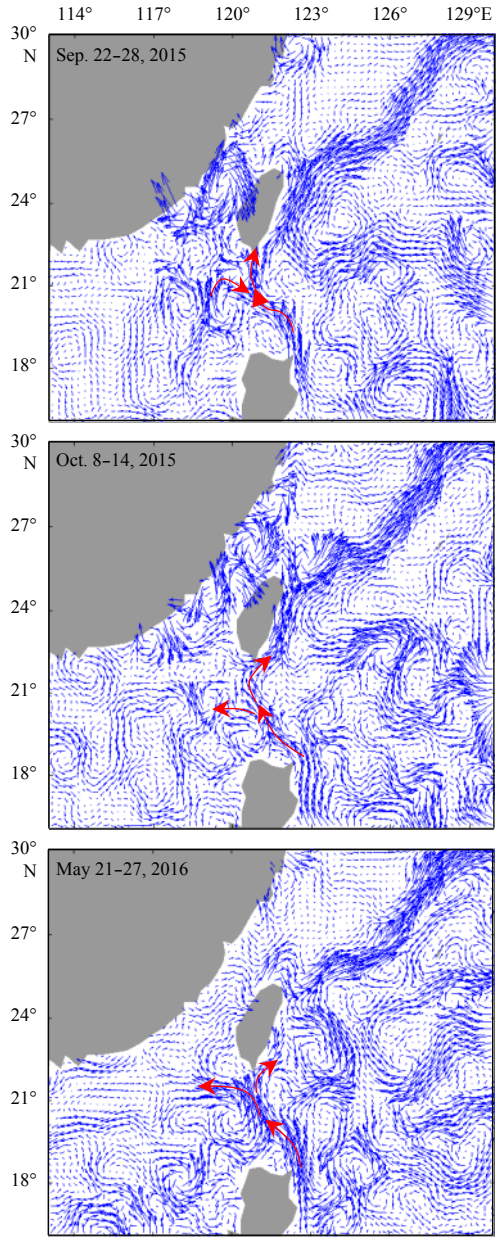

Fig. 6. Geostrophic currents map of the Luzon Strait and its adjacent areas before and after the typhoon in September 2015 and May 2016.

typhoon" sampling areas, and Zone B enclosed by green lines represents the "post-typhoon" sampling areas. Assuming one single sample in the upper mixed layer could represent the whole mixed layer (Moore, 2007), we designed an orthogonal horizontal linear grid to map the two zones with special scale of 10 km× 10 km. The observed ^{224}Ra and ^{137}Cs activities were interpolated to the grid cells by the Kriging method, and then the inventories of both nuclides (Bq) for each zone was the sum of the activities multiplied by the depth of the mixed layer (i.e., 50 m) in each grid cell. Table 1 gives the results of ^{224}Ra and ^{137}Cs inventories in the two zones.

The areas of Zone A and Zone B were calculated in the same way to be 5.83×10^{10} m^3 and 5.95×10^{10} m^3, respectively, the averages of both isotopes could be expressed as the ratios of the inventories to the products of the areas and the depths in each zone. Comparing the activities of ^{224}Ra covered by Zone A and Zone B, it was concluded that the activities of ^{224}Ra in the surface water of Zone B were significantly lower than those in Zone A. As shown in Table 1, the average ^{224}Ra activity in Zone A was 0.226 Bq/m^3, while that of Zone B was only 0.080 Bq/m^3. The difference of ^{224}Ra activity in the surface water before and after Typhoon Rainbow might have been caused by two reasons. One is spatial variability of ^{224}Ra activity between Zone A and Zone B, which is expected because the ^{224}Ra activities will be higher closer to land and lower in the open ocean; the other is the typhoon event. To explore the possible reasons, the survey of May 2016, which was not affected by a typhoon, was grouped in the same way. Thus, we were able to conclude that the spatial difference of ^{224}Ra activities between Zone A and Zone B was only 0.037 Bq/m^3 (Table 1). It was far from possible to interpret the difference between before and after the typhoon event in September 2015, therefore, we conclude that Typhoon Rainbow may have had an impact on the activity level of ^{224}Ra in the study area.

According to the variation of the geostrophic flow field in the study area, there was a significant anticyclone in Zone A before Typhoon Rainbow in September 2015, thus, the western Pacific water did not enter the South China Sea when it bypassed the Luzon Strait. Therefore, the South China Sea could retain its composition and flow eastward into the Philippine Sea. Because the South China Sea is close to the mainland of China, it maintained a relatively high ^{224}Ra activity as it avoided the dilution of the western Pacific water. However, the western Pacific water passed through the Luzon Strait as a cyclone when the typhoon occurred. A large amount of the western Pacific water characterized by low ^{224}Ra activity had flooded into the South China Sea, reducing the activity of ^{224}Ra in the study area. Considering that the geostrophic flow field in May 2016 was roughly similar to that after the typhoon occurred, we took the survey of May 2016 as an example to explore the impact of the typhoon on ^{224}Ra activity in the surface water of the study area. The activity of seawater ^{224}Ra in Zone A was significantly lower than the average level of the same region in the previous survey, which suggested that Typhoon Rainbow might have an important dilution effect on decreasing the activities of ^{224}Ra in the South China Sea.

Here we clarify that since any change in ^{224}Ra that occurred from the typhoon would be reset after about one month (about six half-lives of ^{224}Ra), and any new typhoon event never occurred during the survey of May 2016, the low ^{224}Ra activities observed in May 2016 were not in fact from the typhoon, but rather from the same circulation pattern as that after Typhoon Rainbow in September 2015. This kind of circulation is driving the low

Table 1. Comparison of the average activities of ^{224}Ra and ^{137}Cs between Zone A and Zone B during both cruises

Cruise		Zone A (5.83×10^{10} m^3)		Zone B (5.95×10^{10} m^3)	
		Inventory/10^{11} Bq	Average/Bq·m^{-3}	Inventory/10^{11} Bq	Average/Bq·m^{-3}
September 2015	^{224}Ra	6.58	0.226	2.38	0.080
	^{137}Cs	27.30	0.936	27.30	0.917
May 2016	^{224}Ra	4.09	0.140	3.06	0.103
	^{137}Cs	23.00	0.788	26.00	0.874

^{224}Ra activities into the South China Sea, thus it is also important to clarify that this can occur in the absence of typhoon. Furthermore, we also infer that the effect would be magnified with Typhoon Rainbow.

Supposing that the ^{137}Cs activity of the surface water were grouped in the same form as ^{224}Ra, the calculation would be totally different from that of ^{224}Ra: the average activities of ^{137}Cs before and after the typhoon were around 0.9 Bq/m^3 in the survey of September 2015. Meanwhile, the average activities of ^{137}Cs in Zone A were also close to Zone B in May 2016. The similarity indicates that there was no significant difference in the activity of ^{137}Cs between the western Pacific Ocean and the South China Sea. This result may be explained by the fact that ^{137}Cs, as a longer half-life nuclide, does not have the short-term behavior that ^{224}Ra does, therefore, the long-term migration and mixing processes of water in the South China Sea and the West Pacific Ocean might have made the ^{137}Cs activities relatively consistent, and thus the ocean current reversal phenomenon caused by the typhoon event might not have affected the ^{137}Cs activity of the water in the study area.

5 Conclusions

During the cruises of September 2015 and May 2016, $^{224, 223}$Ra and ^{137}Cs were analyzed in the Luzon Strait and its adjacent waters. The results showed that the activities of $^{224, 223}$Ra and ^{137}Cs in surface water of the Luzon Strait and its adjacent waters were within the range of 0.017–0.358 mBq/L, undetected to 0.013 mBq/L, and 0.58–1.27 mBq/L, respectively. The activities of ^{224}Ra and ^{137}Cs in stratified samples of LS3, LS5 and LS8 were within the range of 0.009–0.084 mBq/L and 0.26–1.96 mBq/L, respectively. From west to east along the Luzon Strait, the ^{224}Ra activity was observed to gradually increase from the northern South China Sea to the Philippine Sea. The ^{137}Cs had no large spatial distribution characteristics and had no variation compared with historical data. Based on the vertical distributions of ^{224}Ra and ^{137}Cs at the three stations (LS3, LS5 and LS8), the tropical surface water (TSW) was observed to have a higher activity and a greater gradient change of ^{224}Ra, whereas ^{137}Cs had lower activity and a lower gradient change. The activities of ^{224}Ra in both the subsurface water (SSW) and the intermediate water and deep water (I&DW) were much lower but relatively stable. By contrast, the activities of ^{137}Cs were somewhat higher and the gradients changed greatly in both of the water masses. The subsurface water of Sta. LS8 located in the Philippine Sea might have submerged into the layer of the intermediate water mass, which increased the activities of ^{224}Ra and ^{137}Cs at the water depth of 600 m. Typhoon Rainbow caused the overall current circulation around the Luzon Strait to be reversed. A large amount of western Pacific water characterized by low ^{224}Ra activities flooded into the South China Sea, reducing the activities of ^{224}Ra in the seawater, but the ^{137}Cs had no variation of activity in the study area, which indicated that there was no significant difference in the ^{137}Cs activity between the western Pacific Ocean and the northern South China Sea.

References

Aoyama M, Kajino M, Tanaka T Y, et al. 2016. ^{134}Cs and ^{137}Cs in the North Pacific Ocean derived from the March 2011 TEPCO Fukushima Dai-ichi Nuclear Power Plant accident, Japan. Part two: estimation of ^{134}Cs and ^{137}Cs inventories in the North Pacific Ocean. Journal of Oceanography, 72(1): 67–76

Bailly du Bois P, Laguionie P, Boust D, et al. 2012. Estimation of marine source-term following Fukushima Dai-ichi accident. Journal of Environmental Radioactivity, 114: 2–9, doi: 10.1016/j.jenvrad.2011.11.015

Bronson F L. 2003. Validation of the accuracy of the LabSOCS software for mathematical efficiency calibration of Ge detectors for typical laboratory samples. Journal of Radioanalytical and Nuclear Chemistry, 255(1): 137–141, doi: 10.1023/A:1022248318741

Buesseler K O, Charette M A, Pike S M, et al. 2018. Lingering radioactivity at the Bikini and Enewetak Atolls. Science of the Total Environment, 621: 1185–1198, doi: 10.1016/j.scitotenv.2017.10.109

Charette M A, Breier C F, Henderson P B, et al. 2013. Radium-based estimates of cesium isotope transport and total direct ocean discharges from the Fukushima Nuclear Power Plant accident. Biogeosciences, 10(3): 2159–2167, doi: 10.5194/bg-10-2159-2013

Dulaiova H, Burnett W C. 2008. Evaluation of the flushing rates of Apalachicola Bay, Florida via natural geochemical tracers. Marine Chemistry, 109(3–4): 395–408, doi: 10.1016/j.marchem.2007.09.001

Garcia-Solsona E, Garcia-Orellana J, Masqué P, et al. 2008. Uncertainties associated with ^{223}Ra and ^{224}Ra measurements in water via a Delayed Coincidence Counter (RaDeCC). Marine Chemistry, 109(3–4): 198–219, doi: 10.1016/j.marchem.2007.11.006

Gu Hequan. 2015. A quantitative study on the sources and sinks of radium isotopes in near-shore waters—taking Changjiang estuary and its adjacent offshore area, Bamen Lagoon, Gaolong Bay and Boao Bay in Hainan for example (in Chinese) [dissertation]. Shanghai: East China Normal University

Hancock G J, Webster I T, Stieglitz T C. 2006. Horizontal mixing of Great Barrier Reef waters: Offshore diffusivity determined from radium isotope distribution. Journal of Geophysical Research, 111(C12): C12019, doi: 10.1029/2006JC003608

Liu Qinyu, Yang Haijun, Li Wei, et al. 2000. Velocity and transport of the zonal current in the Luzon Strait. Haiyang Xuebao (in Chinese), 22(2): 1–8

Moore W S. 1976. Sampling ^{228}Ra in the deep ocean. Deep Sea Research and Oceanographic Abstracts, 23(7): 647–651, doi: 10.1016/0011-7471(76)90007-3

Moore W S. 2000. Ages of continental shelf waters determined from ^{223}Ra and ^{224}Ra. Journal of Geophysical Research, 105(C9): 22117–22122, doi: 10.1029/1999JC000289

Moore W S. 2007. Seasonal distribution and flux of radium isotopes on the southeastern U. S. continental shelf. Journal of Geophysical Research, 112(C10): C10013, doi: 10.1029/2007JC004199

Moore W S, Arnold R. 1996. Measurement of ^{223}Ra and ^{224}Ra in coastal waters using a delayed coincidence counter. Journal of Geophysical Research, 101(C1): 1321–1329, doi: 10.1029/95JC03139

Moore W S, Krest J. 2004. Distribution of ^{223}Ra and ^{224}Ra in the plumes of the Mississippi and Atchafalaya rivers and the Gulf of Mexico. Marine Chemistry, 86(3–4): 105–119, doi: 10.1016/j.marchem.2003.10.001

Pan Yuqiu. 2005. China offshore water masses. In: Su Jilan, Yuan Yeli, eds. China Offshore Hydrology (in Chinese). Beijing: China Ocean Press, 167–169

Stachelhaus S L, Moran S B, Ullman D S, et al. 2012. Cross-shelf mixing and mid-shelf front dynamics in the Mid-Atlantic Bight evaluated using the radium quartet. Journal of Marine Research, 70(1): 141–172, doi: 10.1357/002224012800502426

Wu J W, Zhou K B, Dai M H. 2012. Impacts of the Fukushima nuclear accident on the China Seas: evaluation based on anthropogenic radionuclide ^{137}Cs. Chinese Science Bulletin (in Chinese), 57(32): 3100–3108, doi: 10.1007/s11434-012-5426-2

Zhou P, Li D M, Zhao L, et al. 2018. Radioactive status of seawater and its assessment in the northeast South China Sea and the Luzon Strait and its adjacent areas from 2011 to 2014. Marine Pollution Bulletin, 131: 163–173, doi: 10.1016/j.marpolbul.2018.04.009